cis–trans Isomerisation of Substituted Aromatic Imines: A Comparative Experimental and Theoretical Study

ARTICLE *in* CHEMPHYSCHEM · AUGUST 2011

Impact Factor: 3.42 · DOI: 10.1002/cphc.201100179 · Source: PubMed

DOI: 10.1002/cphc.201100179

cis–trans Isomerisation of Substituted Aromatic Imines: A Comparative Experimental and Theoretical Study

Ying Luo,[a] Manuel Utecht,[b] Jadranka Dokić,[a] Sergey Korchak,[c] Hans-Martin Vieth,[c] Rainer Haag,*[a] and Peter Saalfrank*[b]

The *cis–trans* isomerisation of *N*-benzylideneaniline (NBA) and derivatives containing a central C=N bond has been investigated experimentally and theoretically. Eight different NBA molecules in three different solvents were irradiated to enforce a photochemical *trans*$\xrightarrow{h\nu}$*cis* isomerisation and the kinetics of the thermal backreaction *cis*$\xrightarrow{\Delta}$*trans* were determined by NMR spectroscopy measurements in the temperature range between 193 and 288 K. Theoretical calculations using density functional theory and Eyring transition-state theory were carried out for 12 different NBA species in the gas phase and three different solvents to compute thermal isomerisation rates of the thermal back reaction. While the computed absolute rates are too large, they reveal and explain experimental trends. Time-dependent density functional theory provides optical spectra for vertical transitions and excitation energy differences between *trans* and *cis* forms. Together with isomerisation rates, the latter can be used to identify "optimal switches" with good photochromicity and reasonable thermal stability.

1. Introduction

Reversible photo-induced *cis–trans* isomerisation of organic molecules, such as azobenzene derivatives, has long been well known.[1] This type of isomerisation causes the molecule to switch between two states with different chemical and physical properties. Recently, these photo-sensitive systems were mounted on solid surfaces either by chemisorption, in an upright position,[2–5] or physisorption, in which case scanning tunnelling microscopy (STM)[6,7] or optically[8] induced *cis–trans* isomerisations of molecules lying flat on the surface have already been observed. These results show the capabilities of these systems to act as nanoscale molecular motors.[9]

Another photo-sensitive functional group, imine (C=N), is a potential alternative to the diazo (N=N) switch under certain conditions. In the 1970s, the conformations of the thermodynamically most stable *trans*-benzylideneaniline derivatives (see Figure 1) were investigated in the solid state by X-ray crystallography.[10,11] In most cases, these molecules are nonplanar, with torsion angles β (see Figure 1) of the aniline ring out of the molecular plane of 41–55°, depending on the species, while the phenyl ring in the benzylidene moiety just slightly twists in the opposite direction. In contrast, *trans*-diazobenzenes are planar. To avoid imperfections caused by intermolecular forces in the crystalline state, studies in solution and in the gas phase by electronic absorption spectroscopy[12,13] and electron diffraction[14] were carried out, giving similar results. Different kinds of theoretical calculations also demonstrated the nonplanar conformation of *trans*-NBA derivatives.[15]

The photo-isomerisation of a C=N double bond was originally inferred by Kuhn and Weitz to explain a reversible colour change resulting from irradiation of triphenylformazan.[16] The first spectroscopic observation of the *trans*→*cis* photo-isomerisation of imines was reported by Fischer and Frei in 1957, through a significant change of the absorption spectrum in solution after photo-irradiation at −100 °C.[17] The spectra of the

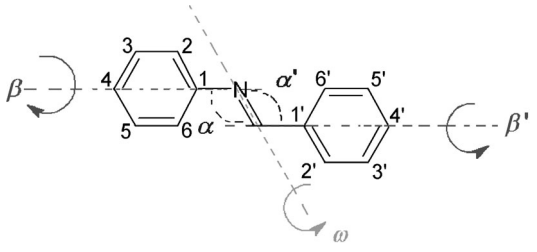

Figure 1. Schematic representation of *N*-benzylideneaniline (NBA) with numbering of atom positions and definition of angles and dihedrals used in the text. β is the dihedral angle formed by atoms C_2, C_1, N, and C (central); β' is the dihedral angle formed by atoms $C_{6'}$, $C_{1'}$, C (central), and N; ω is the dihedral angle formed by atoms C_1, N, C (central), and $C_{1'}$; α is the angle between atoms C_1, N, and C(central); α' is the angle between atoms N, C (central), and $C_{1'}$.

[a] *Y. Luo, Dr. J. Dokić, Prof. Dr. R. Haag*
Freie Universität Berlin
Institut für Chemie und Biochemie
Takustraße 3, D-14195 Berlin (Germany)
Fax: (+49) 30-838-53357
E-mail: haag@chemie.fu-berlin.de

[b] *M. Utecht, Prof. Dr. P. Saalfrank*
Universität Potsdam
Institut für Chemie
Karl-Liebknecht-Straße 24–25, D-14476 Potsdam-Golm (Germany)
Fax: (+49) 331-977-5058
E-mail: petsaal@rz.uni-potsdam.de

[c] *Dr. S. Korchak, Prof. Dr. H.-M. Vieth*
Freie Universität Berlin
Institut für Experimentalphysik
Arnimallee 14, D-14195 Berlin (Germany)

Supporting information for this article is available on the WWW under http://dx.doi.org/10.1002/cphc.201100179.

original isomer were restored with raising the temperature. The activation energy for this thermal, *cis*→*trans* process is around 70 kJ mol^{-1}, which is appreciably lower than those for azobenzene (ca. 95 kJ mol^{-1}) and stilbene (175 kJ mol^{-1}), resulting in a significantly shorter half-life of the *cis* isomer of only about 1 s at 25 °C.[17,18] Later, different experimental methods, such as flash photolysis,[18–20] NMR spectroscopy,[21,22] UV/Vis spectroscopy[23] and IR spectroscopy,[24] were applied for further studies of this isomerisation process, including substituent[18–21,23,25] and solvent effects.[19,20,25]

Moreover, for deeper analysis, semi-empirical [complete neglect of differential overlap (CNDO)] molecular orbital,[13,15] ab initio,[20] and density functional calculations[25,26] were performed. It was suggested that the photochemical *trans*→*cis* isomerisation was achieved by out-of-plane rotation around the C=N double bond, whereas thermal back relaxation proceeded by in-plane nitrogen inversion through a linear transition state (TS).[9]

For the *cis*→*trans* thermal isomerisation, Asano and coworkers investigated several types of imine compounds by high-pressure ^{19}F NMR spectroscopy measurements[22] and theoretical computations,[25c] and suggested two different inversion pathways. It was found that the TS geometry changed with different substituents in the 4-position of aniline (see Figure 1). If the substituent is an electron-donor group, the aromatic ring in aniline is coplanar with the R^1R^2C=N double-bond plane at the TS, suggesting a planar inversion pathway. (In the case of NBA compounds, we have R^1=H and R^2= phenyl.) On the contrary, when the substituent is electron withdrawing, a TS with two planes perpendicular to each other is favoured.

These findings suggest that substituents and possibly also solvent effects are key determinants for the switching of NBA species. Details, however, are still not well known. Therefore, before systematic studies for reversible isomerisation of imines on surfaces can be started, one should further and better understand the isomerisation mechanism in solution. For this purpose, herein, the *cis*→*trans* thermal isomerisation kinetics of NBA derivatives are studied in light of theoretical calculations and NMR spectroscopy experiments, with special attention on a systematic investigation of substituent and solvent effects. Aside from general 4- and 4′-double-substituted NBA compounds, some push–pull systems and molecules with bulky substituents are studied as well. We also calculate optical spectra for *trans* and *cis* isomers using vertical excitations; this way the ability of the molecules to be selectively and reversibly switched by photons of different energies is estimated. This allows the identification of optimal NBA switches, which are photochromic and at the same time thermally as stable as possible.

Experimental Section and Computational Methods

Systems Studied: Various NBA derivatives were investigated. Table 1 lists all species that were studied quantum chemically. For compounds **1** to **8**, low-temperature NMR spectroscopy experiments were carried out additionally to determine reaction rates.

Table 1. Structural formulae of (substituted) NBA molecules (*trans* forms) investigated in this work. Abbreviations: NBA = (*N*-)benzylideneaniline, TBI = *tert*-butyl-NBA, TMNBA = tetramethyl-NBA, 4-X-4′-Y denotes double-substituted (in the 4- and 4′-positions) NBA.

	molecule	formula		molecule	formula
1	4-Me-4′-Me	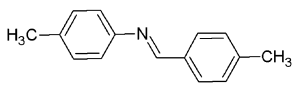	**7**	TMNBA	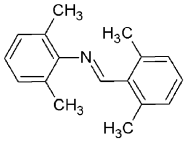
2	4-CN-4′-CN	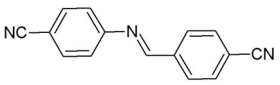	**8**	TBI	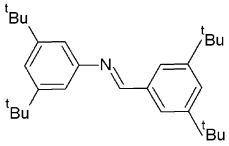
3	4-OMe-4′-CN	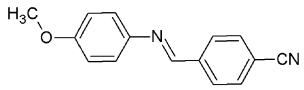	**9**	4-Me-4′-OMe	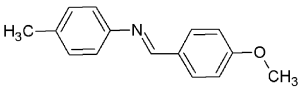
4	4-CN-4′-OMe	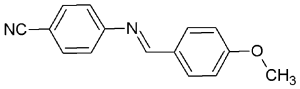	**10**	4-OMe-4′-OMe	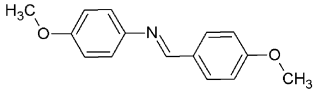
5	4-Me-4′-CN	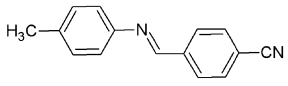	**11**	4-OMe-4′-Me	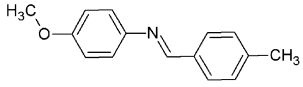
6	4-CN-4′-Me	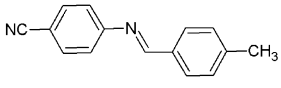	**12**	NBA	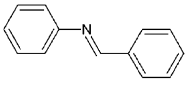

Most molecules studied herein are double substituted in the 4- and 4′-positions (see Figure 1), with donors (–O–Me as a π donor or –Me as a σ donor) or an acceptor (–CN as a π acceptor). For **7** and **8**, four (bulky) alkyl groups have been placed in various positions. Unsubstituted NBA (**12**) serves as a reference.

In experiments, three different solvents were considered, namely, acetone as the "standard" with a dielectric constant of $\varepsilon = 20.49$; THF ($\varepsilon = 7.52$) and methanol ($\varepsilon = 32.61$) were used as examples for less and more polar solvents, respectively. In the calculations, also the gas phase (vacuum) was considered as a reference.

Experiment: The imines **1**–**8** were produced by condensation reactions of corresponding anilines and benzaldehydes in p.a. methanol. Afterwards, recrystallisations from p.a. ethanol were performed to obtain pure products. All final products were characterised by ^{1}H NMR spectroscopy, EI-MS and elementary analysis. Details are given in the Supporting Information.

The photochemical and thermal isomerisations of imine compounds were measured by using an NMR spectrometer with 7 T magnets. The probe head with a low-temperature option was modified to allow for sample irradiation, using a quartz light guide. The experiment was done in the following way: The sample was cooled to a target temperature. Before irradiation, an NMR spectrum was taken for the *trans* form of the imine compound. Afterwards light irradiation was applied, using a UV LED with 55 mW power output and a wavelength of 375 nm. After 5 min, the spectrum under constant irradiation was taken. The *cis*/*trans* ratios, which were not optimised, obtained from these spectra vary between 15/85 (compound **1**, $T = 213$ K) and 62/38 (compound **4**, $T = 203$ K). Then, irradiation was switched off and spectra were continuously recorded to monitor the decay of the *cis* form to the *trans* form and to determine the lifetime, τ, and consequently the *cis*→*trans* rate constant, $k = \tau^{-1}$. Due to the small concentration of compounds the spectra were averaged. Each point in the kinetics consists of several averaged spectra. The number of scans varied with the solution, ranging from 4 to 128.

To illustrate the procedure, in Figure 2a the NMR spectra of **2** with and without irradiation are shown. The spectrum of the *cis* isomer can be derived from the spectrum under irradiation by deduction of the scaled spectrum of the *trans* isomer. The *cis*→*trans* rate constant is obtained by a mono-exponential fit of the *cis* isomer decay after the end of irradiation (Figure 2b). An assignment of NMR spectroscopy signals is given in the Supporting Information.

In our experiments, temperatures between 193 and 288 K were considered. However, for an individual molecule and solvent, only a narrow temperature range was studied (of ≈20–40 K); typically three temperatures per compound and solvent. From the rates and temperature dependence, Arrhenius prefactors, *A*, and activation energies, E_a, could be estimated from Equation (1):

$$k = Ae^{-E_a/RT} \tag{1}$$

using an Arrhenius plot ln(*k*) versus 1/*T*. Due to the narrow temperature range per sample, however, the resulting E_a and *A* values are inaccurate and, in some cases, even unphysical, so we report only the directly determined experimental rate constants in the following discussion.

Theory: All calculations were carried out with the Gaussian 09 program package,[27] using hybrid density functional theory (DFT) with the B3LYP exchange-correlation functional,[28] and a 6-31G* basis set.[29]

Thermal isomerisation was studied quantum chemically by Eyring's TS theory,[30] using the same protocol as that given in reference [31]. Accordingly, *cis*→*trans* thermal rate constants are calculated by using Equation (2):

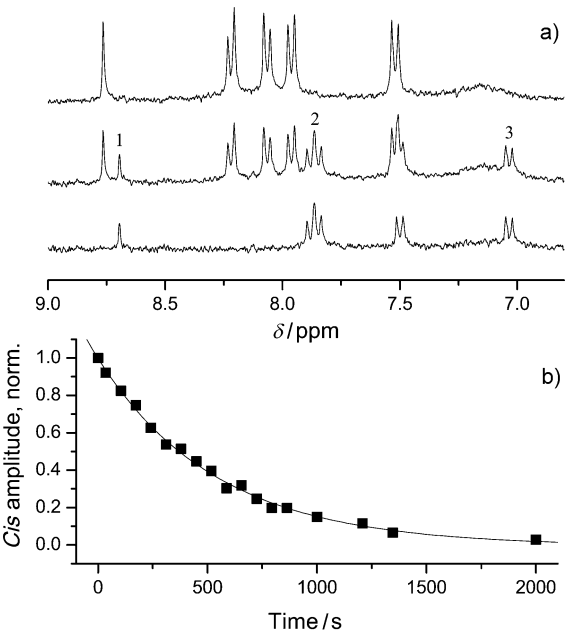

Figure 2. a) ^{1}H NMR spectra of **2** without irradiation (top) (*trans* isomer), during irradiation (middle) and the spectrum of the *cis* isomer (bottom) derived from the middle spectrum by subtraction of the scaled *trans* isomer spectrum. b) Decay of non-overlapping lines of the *cis* isomer (1,2,3) after irradiation in [D_6]acetone at 213 K.

$$k(T) = \frac{k_B T}{h} e^{-\Delta G^{\ddagger}/RT} \tag{2}$$

in which $\Delta G^{\ddagger}$ is the activation free energy, that is, $\Delta G^{\ddagger} = G^{\ddagger} - G_c$ for the *cis*→*trans* reaction ($\ddagger$ denotes the TS, *c* the *cis* form). Reactant (e.g., *cis*) and product minima (e.g., *trans*) were determined and the minimum character was verified by the fact that normal mode analysis gave only real frequencies. TSs connecting reactants and products were found by the synchronous transit-guided quasi-Newton method (QST2 and QST3),[32,33] and were characterised by a single, imaginary frequency, $i\omega^{\ddagger}$.

We calculated $\Delta G^{\ddagger}$ as $\Delta G^{\ddagger} = \Delta H^{\ddagger} - T\Delta S^{\ddagger}$, in which $\Delta S^{\ddagger}$ is the activation free entropy and $\Delta H^{\ddagger}$ the activation enthalpy. The temperature dependence of $\Delta S^{\ddagger}$ was neglected, that is, we set $\Delta S^{\ddagger} = \Delta S^{\ddagger}(T_0)$, in which T_0 is a reference temperature, chosen as 298.15 K. The temperature dependence of $\Delta H^{\ddagger}$ was approximated as $\Delta H^{\ddagger} = \Delta H^{\ddagger}(0) + T\Delta C_v(T_0)$ from the zero-point-energy (ZPE)-corrected enthalpy $\Delta H^{\ddagger}(0) = \Delta E^{\ddagger} + \Delta E^{\ddagger}_{ZPE}$ at $T = 0$ K (ΔE is a difference of self-consistent field (SCF) energies), and the heat capacity, C_v, at constant volume and at temperature T_0. By analysing an Arrhenius plot of ln*k* versus 1/*T*, we obtained linear functions from which (effective) activation energies, E_a, and prefactors, *A*, as defined by Equation (1) could be determined.

To estimate tunnelling contributions to the rate, in some cases Wigner's one-dimensional correction was used, giving a rate enhancement factor [Eq. (3)]:[34]

$$\Gamma = 1 + \frac{1}{24}\left(\frac{\hbar\omega^{\ddagger}}{kT}\right)^2 \tag{3}$$

in which $\omega^{\ddagger}$ is the (imaginary) TS frequency defined above.

Solvent effects are included in an approximate way only by using the polarisable continuum model (PCM).[35] That is, the molecules under investigation are embedded in a polarisable continuum, characterised by a dielectric constant, ε, characteristic for the solvent of interest. As a continuum model, PCM does not account for the detailed effects of the solvent on a molecular level, but only for electronic polarisation. In particular, rearrangement of solvent molecules during the formation of the TS is neglected. In a more sophisticated treatment of solvent molecules, and possibly also their thermal motion, should be explicitly included. This is, however, beyond the scope of this paper. Gas-phase models are used as a reference in addition to the PCM calculations.

Vertical UV/Vis absorption spectra for reactant and product molecules were calculated from linear-response, time-dependent DFT (TD-B3LYP).[36] To make closer contact with experimental results and to account for line broadening, the stick spectrum was broadened by normalised Gaussians. Accordingly, the extinction coefficients were calculated by Equation (4):

$$\varepsilon(\tilde{\nu}) = \sum_i \frac{f_i}{\kappa\sigma\sqrt{2\pi}} e^{-\frac{1}{2}\left(\frac{\tilde{\nu}-\tilde{\nu}_i}{\sigma}\right)^2} \quad (4)$$

in which $\tilde{\nu} = 1/\lambda$ is the wavenumber, $\kappa = 4.319 \times 10^{-10}\,\mathrm{mol\,m^{-1}}$, f_i is the oscillator strength for transition i, $\tilde{\nu}_i$ the corresponding transition wavenumber and σ is an empirical broadening factor.

2. Results and Discussion

2.1. Energetics and Geometries of Stationary Points

2.1.1. Geometries

Figure 3 shows gas-phase geometries of stationary points (*trans* and *cis*, TS) for the example of compound **2** (4-CN-4′-CN) obtained by B3LYP/6-31G* geometry optimisation and a TS search.

The first finding is that the *cis* form is more non-planar than the *trans* form, similar to azobenzenes .[31] In contrast to those, however, *trans*-**2** is not entirely flat. Rather, the aniline ring rotates out-of-plane as expected from experimental results.[10,11,14] We find $\beta = 145.9^\circ$, which corresponds to a rotation of $180^\circ - \beta = 34.1^\circ$ of the aniline ring out of the plane spanned by $C_{1'}$, C(central) and N (see Figure 1). As shown in Table 2, for the different NBA species, the dihedral angle β varies between 151.7° for *trans*-**3** (4-OMe-4′-CN) and 110.2° for *trans*-**7** (TMNBA), corresponding to out-of-plane angles between 28.3° and 69.7°. The clear non-planarity of TMNBA is due to steric overcrowding at the imine bridge. In contrast to the aniline ring, the phenyl ring in the benzylidene moiety remains always almost in-plane, with dihedral angles β' close to zero—the largest deviation again for TMNBA.

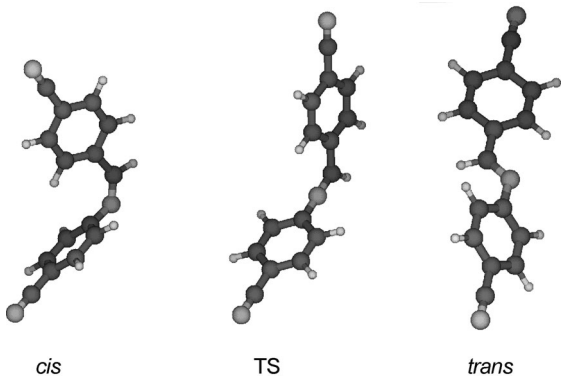

Figure 3. Gas-phase B3LYP/6-31G* geometries for **2** in *cis*, TS, and *trans* forms.

The computed dihedral angles and angles are in reasonable agreement with experimental values, where available. For *trans*-NBA, for example, the out-of-plane rotation of the aniline ring is 39.4° in theory, and 55.2° according to X-ray data.[11] In both cases, the benzylidene ring is only slightly rotated in opposite direction. Also, (gas-phase) bond lengths are in reasonable agreement with (solid-state) bond lengths, and are not listed herein. It is sufficient to note that for *trans*-NBA, for example, we find experimental[11] and theoretical (B3LYP/6-31G*, in brackets) bond lengths of $R_{N=C} = 1.231$ (1.288), $R_{N-C1} = 1.460$ (1.406) and $R_{C-C1'} = 1.496$ Å (1.468 Å), respectively. (Numbering as shown in Figure 1; C without a number denoting the central C atom.)

No experimental information is available for TSs. According to calculations, in the TS, the C1–N=C unit becomes almost linear ($\alpha = 178.9^\circ$ in the case of compound **2**), while the

Table 2. Selected B3LYP/6-31G* angles and dihedral angles for stationary points of (substituted) NBA molecules in the gas phase. All angles are in degrees.

		cis					*trans*					TS			
		ω	β	β'	α	α'	ω	β	β'	α	α'	β	β'	α	α'
1	4-Me-4′-Me	5.3	72.5	15.0	125.3	132.7	177.2	147.6	1.7	120.2	122.8	90.0	0.3	180.0	126.0
2	4-CN-4′-CN	5.1	74.2	15.9	126.7	132.0	177.1	145.9	0.8	120.4	122.3	89.9	0.1	178.9	125.6
3	4-OMe-4′-CN	8.1	57.0	24.0	125.0	132.2	177.5	151.7	0.9	121.1	122.0	135.6	0.1	180.0	125.5
4	4-CN-4′-OMe	2.4	86.5	4.5	127.1	132.8	176.4	142.5	1.3	120.6	123.0	90.0	0.0	180.0	126.2
5	4-Me-4′-CN	6.8	65.0	21.5	125.0	132.0	177.4	148.1	0.9	120.7	122.0	104.0	1.3	180.0	125.4
6	4-CN-4′-Me	3.0	83.2	8.0	127.1	132.6	176.8	141.8	0.7	120.2	122.9	90.1	0.5	179.2	126.1
7	TMNBA	4.3	60.1	52.6	127.3	132.6	178.8	110.2	5.2	119.0	125.6	73.2	14.0	177.7	128.2
8	TBI	1.7	90.4	6.6	126.2	133.1	177.8	146.6	0.5	122.7	122.4	88.6	0.5	180.0	125.9
9	4-Me-4′-OMe	4.7	76.1	11.0	125.4	133.0	177.0	145.4	1.3	120.1	123.0	105.1	6.3	179.8	126.2
10	4-OMe-4′-OMe	6.7	66.5	16.6	124.8	132.9	177.1	147.6	1.3	120.4	122.9	61.2	0.4	178.8	126.1
11	4-OMe-4′-Me	7.2	62.6	19.7	124.9	132.8	177.1	148.1	1.1	120.5	122.7	115.5	0.8	180.0	126.0
12	NBA	4.7	74.9	14.4	125.5	132.7	177.2	143.9	1.2	120.1	122.7	90.2	0.1	180.0	125.9

N=C–C1′ unit does not deviate much from the ideal 120° value ($\alpha' = 125.6°$). The results in Table 2 demonstrate that this is a general finding for all imines studied herein, suggesting that an inversion mechanism (rather than rotation around ω) takes place during thermal isomerisation. The TSs of individual compounds can nevertheless be quite different. This can be monitored by the difference $\beta - \beta'$. If this difference is about 0°, both aromatic rings are in the same plane (planar TS), whereas for $\beta - \beta' \approx 90°$ we have a perpendicular TS with orthogonal benzene rings instead.[25] For compound **2**, the TS is "perpendicular" ($\beta - \beta' = 89.8°$). This is consistent with the suggestion made in reference [22] that energy-withdrawing groups at the 4-position favour perpendicular rings. Note that according to Table 2 all compounds with cyano groups in 4-position (**2**, **4** and **6**) share this feature, with $\beta - \beta' \approx 90°$. From Table 2 we note that the other statement—that electron-donating groups in 4-position favour planar TS geometries—is only partly supported: Those compounds with methoxy groups in the 4-position (**3**, **10**, and **11**) have values of around $\beta - \beta' \approx 60°$ (or 120°), that is, they are indeed more, but not entirely, planar. The same holds true for the sterically demanding **7**, whereas all remaining imines **1**, **5**, **8**, **9** and **12** (i.e., also those with 4-methyl), favour perpendicular TSs.

Solvent effects on geometries were small. We recalculated stationary points using the PCM model with parameters for THF, acetone and methanol. The biggest geometry changes occurred when going from the gas phase to THF ($\varepsilon = 7.43$, see above). Further increasing the dielectric constant in acetone and methanol had no significant additional effect. For completeness, in Table 3 we demonstrate the influence of a solvent (THF) on the dihedral angles ω for the *cis*- and *trans*-NBA molecules **1**–**12**. The biggest solvent effect is observed for *cis*-4-CN-4′-Me, in which the central C–N=C–C unit becomes slightly non-planar.

Table 3. Influence of a solvent (THF) on the dihedral ω (in °) of (substituted) NBA molecules.

		cis		*trans*	
		Gas	THF	Gas	THF
1	4-Me-4′-Me	5.3	5.5	177.2	177.3
2	4-CN-4′-CN	5.1	5.5	177.1	177.0
3	4-OMe-4′-CN	8.1	8.3	177.5	177.6
4	4-CN-4′-OMe	2.4	0.6	176.4	176.7
5	4-Me-4′-CN	6.8	7.0	177.4	177.5
6	4-CN-4′-Me	3.0	10.5	176.8	176.9
7	TMNBA	4.3	4.2	178.8	179.5
8	TBI	1.7	2.9	177.8	177.3
9	4-Me-4′-OMe	4.7	4.8	177.0	177.1
10	4-OMe-4′-OMe	6.7	6.6	177.1	177.2
11	4-OMe-4′-Me	7.2	7.1	177.1	177.2
12	NBA	4.7	5.1	177.2	177.3

2.1.2. Energies

In the gas phase, *trans*-NBAs are found, at the B3LYP/6-31G* level of theory, to be more stable than the *cis* isomers by between 0.238 (23.0) and 0.337 eV (32.5 kJ mol^{-1}). This can be seen from Table 4, where the energy differences $E_c - E_t$ (SCF energies, no zero-point or temperature corrections) are listed. The energy differences are about half those of the typical values found for azobenzenes.[31]

From Table 4 we also note that solvent effects are small when studied by PCM. (Only values for acetone and THF are shown.) The largest difference between the gas phase and THF is found for 4-CN-4′-CN, in which the solvent stabilises *cis* versus *trans* by 0.016 eV (1.5 kJ mol^{-1}). This is due to a large dipole moment of the *cis* form, which is stabilised by the polarisable environment.

The "naked activation energies" for *cis*→*trans* isomerisation (SCF energy differences $E^{\neq} - E_c$) are also listed in Table 4. They are between 0.498 (48.1) and 0.647 eV (62.4 kJ mol^{-1}) in the gas phase. The reference value of unsubstituted NBA is 0.589 eV (56.8 kJ mol^{-1}). These values are quite low when compared with those found for azobenzenes (typically 1 eV),[31] in agreement with earlier work as mentioned above. Note that there are clear substituent effects: For compound **4** (4-CN-4′-OMe), the barrier is 0.498 eV, whereas it is 0.634 eV for compound **3** (4-OMe-4′-CN), in which the substituents at 4- and 4′-positions have been swapped. This shows that (π) acceptors in the 4-position (at the aniline ring), tend to lower activation energies, whereas (π) donors tend to enhance it. This can be explained in simple terms with ionic mesomeric structures, which show that electron acceptors in the *para* position of the aniline ring can stabilise the linear C–N=C unit of the TS—see the analogous arguments in reference [31] for azobenzenes.

From Table 4, we note that there is an influence of the solvent on energy differences $E^{\neq} - E_c$. In THF, the barrier is typically lowered, by up to 0.19 eV (18.3 kJ mol^{-1}) in the case of 4-Me-4′-CN. For acetone (and also for methanol, not shown), the

Table 4. Differences in B3LYP/6-31G* energies for (substituted) NBA molecules in the gas phase and in THF and acetone (in eV).

		Gas phase		THF		Acetone	
		$E_c - E_t$	$E^{\neq} - E_c$	$E_c - E_t$	$E^{\neq} - E_c$	$E_c - E_t$	$E^{\neq} - E_c$
1	4-Me-4′-Me	0.285	0.607	0.278	0.606	0.278	0.630
2	4-CN-4′-CN	0.278	0.504	0.262	0.419	0.260	0.474
3	4-OMe-4′-CN	0.337	0.634	0.330	0.629	0.329	0.672
4	4-CN-4′-OMe	0.238	0.498	0.228	0.428	0.227	0.472
5	4-Me-4′-CN	0.315	0.614	0.307	0.595	0.306	0.632
6	4-CN-4′-Me	0.245	0.498	0.234	0.435	0.284	0.422
7	TMNBA	0.252	0.532	0.247	0.531	0.247	0.531
8	TBI	0.269	0.606	0.266	0.604	0.267	0.629
9	4-Me-4′-OMe	0.279	0.620	0.270	0.605	0.269	0.637
10	4-OMe-4′-OMe	0.302	0.653	0.295	0.642	0.296	0.679
11	4-OMe-4′-Me	0.310	0.647	0.303	0.646	0.303	0.677
12	NBA	0.278	0.589	0.272	0.604	0.273	0.607

classical activation energy can be enhanced or lowered. For compound **3**, for example, the barrier increases by 0.038 eV (3.7 kJ mol^{-1}), whereas for compound **4** it is lowered by 0.026 eV (2.5 kJ mol^{-1}). The overall tendency of the solvent is to stabilise the TS with a linear C–N=C unit, which again can be explained with ionic mesomeric structures.[31] These are stabilised in a polarisable continuum, in particular, if electron acceptors are in the 4-position.

2.2. Reaction Rates for Thermal Isomerisation

2.2.1. Theory

Energy differences, $E^{\neq}-E_c$, have an effect on computed isomerisation rates. Before discussing the results, we checked the quality of the Arrhenius fit [Eq. (1)] compared with rates obtained directly from the Eyring expression [Eq. (2)], and also of other approximations. For this purpose, we show in Table 5 the B3LYP/6-31G* gas-phase rates for all NBA molecules studied in this work, at two different temperatures (298.15 and 213 K, respectively). For $T=298.15$ K, the *cis*→*trans* isomerisation rates obtained directly from the Eyring equation [k_{Eyr}, Eq. (2)] are compared with those obtained from the Arrhenius fit [k_{Arr}, Eq. (1)]. For a selected case (k_{Arr}, $T=298.15$ K), the *trans*→*cis* isomerisation rates are also given.

From Table 5 we note, by comparing the *cis*→*trans* k_{Arr} and k_{Eyr} rates at $T=298.15$ K, that differences are typically in the order of 10%. This shows that the Arrhenius fit is accurate enough to make predictions for other temperatures.

All of the rates in Table 5 are without tunnelling corrections. Using Equation (3), we can estimate the enhancement factor, Γ. For the reference compound, NBA **12**, we find $\hbar\omega^{\neq}=243$ cm^{-1}, giving $\Gamma=1.11$ and 1.06 at $T=213$ and 298.15 K, respectively. Thus, tunnelling corrections are also small and are neglected in the following discussion.

From the results shown in Table 5, we find that the *cis*→*trans* isomerisation rates are between about 3×10^3 and 8×10^4 s^{-1} at room temperature, and between 3×10^{-2} and 5×10^1 s^{-1} at 213 K. This suggests *cis* lifetimes in the millisecond regime at room temperature and still in the range of seconds at the lower temperature. Even the *trans*→*cis* rates are appreciable, in the order of 0.1 s^{-1} for NBA **12** at room temperature. Compared with experiment, at least when performed in solution, the computed rates are several orders of magnitude too large, as discussed in more detail below. Experimental gas-phase isomerisation rates are not available for comparison, to the best of our knowledge.

Focussing on trends predicted by theory, we find that, in particular, those compounds with cyano groups in the 4-position decay quickly, namely, compounds **2**, **4**, and **6**. In contrast compounds **3**, **10** and **11**, with the electron-donating methoxy group in the 4-position, isomerise more slowly. Molecules such as NBA (**12**), TBI (**8**) or 4-Me-4′-Me (**1**), which have no or electronically less active substituents, are in between. An exception to the rule is the sterically demanding TMNBA molecule (compound **7**), with a rate comparable to 4-CN-substituted imines. The decay rates reflect nicely the energy differences $E^{\neq}-E_c$ listed in Table 4. The "effective" E_a values derived from the Equation (1), which are listed in Table 6, show the same trends as the "naked" energy differences. Quantitatively, the effective activation energies, E_a, are typically 0.05 eV (4.8 kJ mol^{-1}) smaller than the bare SCF energy differences, which is mostly due to ZPE corrections.

From the results shown in Table 6, we also find that gas-phase Arrhenius prefactors are in the range between 3×10^{11} and 2×10^{13} s^{-1}. It should be noted, however, that according to Eyring TS theory the prefactors are determined by activation entropies, which can be very inaccurate at the present level of theory.[31]

The results in Table 6 further suggest similar solvent effects for the Arrhenius activation energies, E_a, as those already observed for the bare SCF energy differences, $E^{\neq}-E_c$, as discussed above: For THF, the activation energies tend to be lower than those in the gas phase, whereas for acetone both higher and lower E_a values are found. One would therefore expect that rates behave as $k(\text{gas})\approx k(\text{acetone})<k(\text{THF})$. This is largely supported by theory. For TBI (**8**), for example, the computed rates at $T=253$ K (a temperature that has been considered experimentally, see below), are 5.88×10^1 (gas), 5.23×10^1 (acetone) and 1.70×10^2 s^{-1} (THF). Clearly, the activation energy dominates over prefactors.

In summary, the theoretical rates do not depend much on solvent type (typically by, at most, one order of magnitude), but strongly depend on substitution. In particular, activation energies are strongly substitution dependent.

Table 5. Isomerisation rates of (substituted) NBA molecules (in s^{-1}) at different temperatures, obtained by different theoretical models (Eyring data vs. Arrhenius fit to Eyring data).

		cis→*trans*			*trans*→*cis*
		k_{Arr} 213 K	k_{Eyr} 298.15 K	k_{Arr} 298.15 K	k_{Eyr} 298.15 K
1	4-Me-4′-Me	8.68×10^{-1}	4.78×10^3	5.39×10^3	1.09×10^{-1}
2	4-CN-4′-CN	5.66×10^1	7.51×10^4	8.02×10^4	1.93×10^0
3	4-OMe-4′-CN	1.25×10^{-1}	9.62×10^2	1.17×10^3	2.01×10^{-3}
4	4-CN-4′-OMe	2.85×10^1	5.43×10^4	3.83×10^4	7.67×10^0
5	4-Me-4′-CN	3.37×10^{-1}	2.18×10^3	2.36×10^3	2.30×10^{-2}
6	4-CN-4′-Me	2.80×10^0	4.28×10^3	3.83×10^3	2.01×10^0
7	TMNBA	4.23×10^1	8.14×10^4	9.41×10^4	4.87×10^{-1}
8	TBI	4.60×10^{-1}	2.60×10^3	2.82×10^3	3.78×10^{-2}
9	4-Me-4′-OMe	1.48×10^{-1}	1.08×10^3	1.13×10^3	4.92×10^{-2}
10	4-OMe-4′-OMe	3.51×10^{-2}	4.11×10^2	4.36×10^2	4.13×10^{-3}
11	4-OMe-4′-Me	3.36×10^{-2}	3.64×10^2	3.83×10^2	2.53×10^{-3}
12	NBA	7.23×10^{-1}	3.46×10^3	3.57×10^3	1.20×10^{-1}

2.2.2. Comparison with Experimental Isomerisation Rates

More than 40 *cis*→*trans* rates were measured for compounds **1**–**8** by using NMR spectroscopy. In most cases, acetone was

Table 6. B3LYP/6-31G* Arrhenius activation energies, E_a, and prefactors, A, for (substituted) NBA molecules in the gas phase and in different solvents. All rates in s^{-1}; energies in eV.

		Gas		THF		Acetone	
		E_a	A	E_a	A	E_a	A
1	4-Me-4′-Me	0.561	1.66×10^{13}	0.560	1.95×10^{13}	0.581	2.31×10^{12}
2	4-CN-4′-CN	0.466	6.10×10^{12}	0.384	4.52×10^{12}	0.438	4.39×10^{12}
3	4-OMe-4′-CN	0.587	9.86×10^{12}	0.582	1.09×10^{13}	0.624	1.19×10^{13}
4	4-CN-4′-OMe	0.463	2.56×10^{12}	0.392	3.74×10^{12}	0.436	3.74×10^{12}
5	4-Me-4′-CN	0.569	9.86×10^{12}	0.547	2.53×10^{13}	0.585	2.48×10^{13}
6	4-CN-4′-Me	0.464	2.67×10^{11}	0.401	1.58×10^{13}	0.434	4.27×10^{11}
7	TMNBA	0.495	2.22×10^{13}	0.476	1.99×10^{13}	0.499	1.97×10^{13}
8	TBI	0.560	8.41×10^{12}	0.554	1.85×10^{13}	0.582	2.09×10^{13}
9	4-Me-4′-OMe	0.575	5.92×10^{12}	0.559	4.95×10^{12}	0.591	5.05×10^{12}
10	4-OMe-4′-OMe	0.606	7.61×10^{12}	0.590	4.21×10^{13}	0.627	1.68×10^{13}
11	4-OMe-4′-Me	0.600	5.41×10^{12}	0.595	1.91×10^{13}	0.626	2.09×10^{13}
12	NBA	0.546	6.17×10^{12}	0.559	8.95×10^{12}	0.561	9.12×10^{12}

the solvent used, although in some cases methanol or THF were also used. These rates are listed in Table 7, together with theoretical rates obtained from the Eyring-based E_a and A values described above.

A comparison of experimental and theoretical rates shows that the latter are typically two to five orders of magnitude larger than the former. Isomerisation rates of imines in benzene at room temperature, as determined by other experimental techniques,[20] were in the order of 0.1 to a few hundred s^{-1}, whereas we find typical values of a few hundred to several ten thousand s^{-1} according to Table 5 for the gas phase. For azobenzenes, previous work showed that computed and measured activation energies were in good agreement, while prefactors were not.[31] It is therefore tempting to assume that, also in the present case, the error is dominated by the theoretical prefactor, A, which could be substantially smaller. This can in part be due to inaccuracies in the computed activation entropies, as mentioned above, and, most probably, due to the simplified treatment of the solvent as a polarisable medium, neglecting all "mechanical" effects associated with large-amplitude motions in viscous media.

Closer inspection shows that the absolute activation energies as calculated here may also have to be corrected to achieve quantitative agreement between theory and experiment. In reference [20], the inversion barrier derived from *cis*→*trans* isomerisation of unsubstituted NBA in benzene has been given as 70.1 kJ mol^{-1} (0.73 eV). Since our activation energies for NBA according to Table 6 are around 0.55 eV and not very solvent dependent, we conclude that the

Table 7. Experimental and theoretical *cis*→*trans* rates of (substituted) NBA molecules in solvents at different temperatures (all in s^{-1}).

		Solvent	T [K]	k_{exptl}	k_{theo}
1	4-Me-4′-Me	acetone	213.0	$2.12\pm0.11\times10^{-4}$	4.03×10^{-2}
			223.0	$3.14\pm0.37\times10^{-4}$	1.67×10^{-1}
			233.0	$3.94\pm0.42\times10^{-4}$	6.12×10^{-1}
2	4-CN-4′-CN	acetone	193.0	$1.67\pm0.05\times10^{-4}$	1.56×10^{1}
			203.0	$5.43\pm0.14\times10^{-4}$	5.72×10^{1}
			213.0	$1.92\pm0.12\times10^{-3}$	1.86×10^{2}
3	4-OMe-4′-CN	acetone	223.0	$5.88\pm0.45\times10^{-4}$	9.17×10^{-2}
			228.0	$7.14\pm0.77\times10^{-4}$	1.87×10^{-1}
			233.0	$6.80\pm0.47\times10^{-4}$	3.70×10^{-1}
4	4-CN-4′-OMe	acetone	203.0	$4.55\pm0.10\times10^{-4}$	5.58×10^{1}
			213.0	$3.56\pm0.17\times10^{-3}$	1.80×10^{2}
			223.0	$1.24\pm0.09\times10^{-2}$	5.22×10^{2}
5	4-Me-4′-CN	acetone	233.0	$1.22\pm0.04\times10^{-4}$	5.62×10^{0}
			243.0	$9.80\pm0.90\times10^{-4}$	1.86×10^{1}
			253.0	$4.81\pm0.68\times10^{-3}$	5.62×10^{1}
5	4-Me-4′-CN	methanol	235.0	$1.52\pm0.07\times10^{-4}$	4.66×10^{0}
			248.5	$9.09\pm0.58\times10^{-4}$	2.29×10^{1}
			262.0	$7.30\pm1.26\times10^{-3}$	9.53×10^{1}
6	4-CN-4′-Me	acetone	203.0	$7.14\pm0.15\times10^{-4}$	7.03×10^{0}
			213.0	$5.56\pm0.31\times10^{-3}$	2.25×10^{1}
			223.0	$3.03\pm0.78\times10^{-2}$	6.52×10^{1}
7	TMNBA	acetone	213.0	$2.17\pm0.19\times10^{-4}$	3.11×10^{1}
			223.0	$1.63\pm0.05\times10^{-3}$	1.05×10^{2}
			233.0	$9.43\pm0.63\times10^{-3}$	3.21×10^{2}
8	TBI	acetone	248.0	$6.25\pm0.27\times10^{-4}$	3.05×10^{1}
			253.0	$1.06\pm0.02\times10^{-3}$	5.23×10^{1}
			258.0	$2.72\pm0.10\times10^{-3}$	8.78×10^{1}
			263.0	$5.43\pm0.30\times10^{-3}$	1.44×10^{2}
			268.0	$7.69\pm0.90\times10^{-3}$	2.33×10^{2}
			273.0	$1.11\pm0.04\times10^{-2}$	3.70×10^{2}
			278.0	$2.13\pm0.16\times10^{-2}$	5.78×10^{2}
			283.0	$3.33\pm0.57\times10^{-2}$	8.88×10^{2}
8	TBI	methanol	260.4	$6.31\pm0.28\times10^{-4}$	5.64×10^{1}
			266.0	$1.15\pm0.08\times10^{-3}$	9.83×10^{1}
			273.4	$2.30\pm0.11\times10^{-3}$	1.97×10^{2}
			279.0	$3.91\pm0.11\times10^{-3}$	3.27×10^{2}
			283.0	$6.58\pm0.30\times10^{-3}$	4.63×10^{2}
			288.0	$1.19\pm0.10\times10^{-2}$	7.05×10^{2}
8	TBI	THF	253.0	$5.26\pm0.33\times10^{-4}$	1.70×10^{2}
			258.0	$1.43\pm0.07\times10^{-3}$	2.79×10^{2}
			263.0	$4.55\pm0.31\times10^{-3}$	4.48×10^{2}
			268.0	$1.03\pm0.05\times10^{-2}$	7.06×10^{2}

theoretical activation energies are underestimated, at least when the solvent is treated by our method. In fact, the necessary mechanical work during thermal isomerisation in a viscous medium also increases the activation energy. A barrier increase by 0.73–0.55 = 0.18 eV is a substantial amount for a low-barrier system, such as NBA. It leads to a rate decrease by a factor of about 10^3 at room temperature and a factor of about 2×10^4 at $T = 213$ K, if the same prefactors are assumed. Thus, both prefactors and effective activation energies seem to contribute to the discrepancy between theory and experiment in the case of imines. To account for the solvent properly, one would either have to recalculate the kinetics by explicitly including solvent molecules or by using Kramers' reaction rate theory with friction.[37,38] This is beyond the purpose of the present work.

It must also be noted that experimental results have large error bars because only small temperature ranges could be considered. This makes a comparison between theory and experiment even more difficult. Figure 4, in which the experimental versus theoretical rates of the results given in Table 7 are plotted for **2** and **4**–**8**, shows that at the least trends are consistent. Ideally, if the agreement was complete, one would expect that all points would lie on the line $k_{theo} = k_{exptl}$, that is, a line with a slope of one going through the origin. From analysing Figure 4, we note that there is a clear correlation between measured and computed values and in many cases the theoretical rates for a given molecule increase by about the same order of magnitude as the experimental ones when varying temperature or solvent. General exceptions are molecules **1** and **3**, which lie outside the window shown in Figure 4.

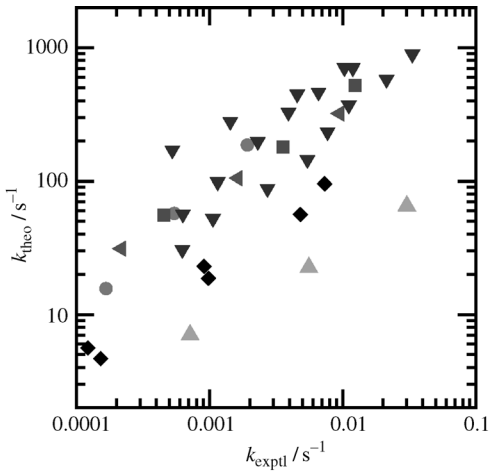

Figure 4. Plot of experimental versus theoretical *cis*→*trans* isomerisation rates for **2** (●), **4** (■), **5** (◆), **6** (▲), **7** (◀) and **8** (▼). See the text for more details.

Inspection of Table 6 and Figure 4 shows that theory and experiment agree with the finding that variation of the solvent has a much smaller effect on the rates than variation of the substituents. For example, at a temperature of 223 K, experimental results suggests compound **4** (4-CN-4′-OMe) isomerises with a rate of 1.24×10^{-2} s^{-1}, whereas compound **3** (4-OMe-4′-CN) has a rate 5.88×10^{-4} s^{-1}. According to theory, the rate changes from 5.22×10^{2} to 9.17×10^{-2} s^{-1}. Similarly, compound **1** (4-Me-4′-Me) isomerises much slower than compound **2** (4-CN-4′-CN) at 213 K. We also note that solvent effects are minor: experimentally, TBI **8** at 268 K isomerises in acetone and THF with experimental rates of about 7.7×10^{-3} and 10.3×10^{-3} s^{-1}, respectively. All of these findings are consistent with the computed activation energies, and the trends expected from there.

2.3. Optical Properties

We also computed absorption spectra of imines, using TD-B3LYP/6-31G* as outlined above. Figure 5a shows a computed spectrum for unsubstituted *trans*-NBA **12** in the gas phase. The broadened spectrum was calculated from vertical transitions by using Equation (4) and a width parameter $\sigma = 2500$ cm^{-1}.

The spectrum shows three signals at around 30000 (ca. 330 or 3.75), 36000 (ca. 275 or 4.5) and 52000 cm^{-1} (ca. 190 nm or 6.5 eV), with the first two merging into a double signal with the low-energy transition being the less intense one. In particular, the lowest-energy absorptions are in good agreement with experimental solution spectra, as reported in references [11] and [13]. In reference [13], for example, the two lowest absorption bands of NBA in cyclohexane were found at 315 ($\varepsilon = 7000$), and 264 nm (17000 L mol^{-1} cm^{-1}), followed by a

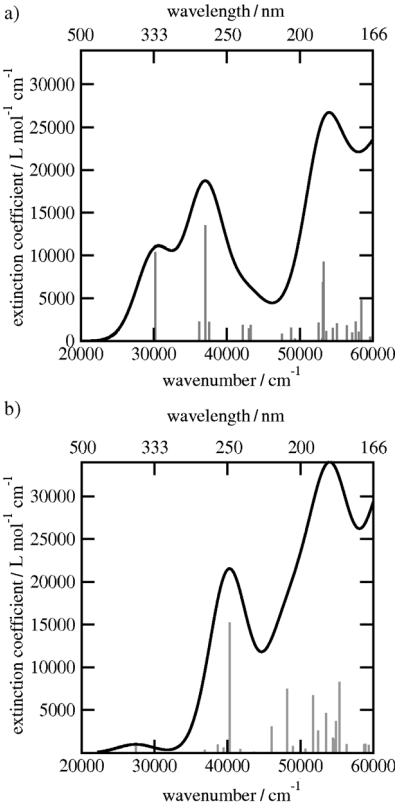

Figure 5. Computed TD-B3LYP/6-31G* vertical absorption spectra of a) *trans*-NBA and b) *cis*-NBA. For smoothed curves, Equation (4) with a broadening parameter of $\sigma = 2500$ cm^{-1} was used. The stick spectra give computed oscillator strengths, f_i, for individual transitions. For *trans*-NBA, the lowest energy absorption has $f = 0.37$, for *cis*-NBA $f = 0.51$.

broad feature with the highest intensity at around 235 nm ($\varepsilon \approx 17\,000\ L\,mol^{-1}\,cm^{-1}$). Theoretical spectra of NBAs have been calculated by the semi-empirical CNDO/S CI method in reference [13], giving low-energy excitation energies that were typically too large.

The lowest-energy signal in the spectrum of *trans*-NBA is dominated by a HOMO→LUMO transition, namely, $\pi \rightarrow \pi^*$, as that found in azobenzene. These two orbitals are depicted in Figure 6. Note that, due to missing molecular symmetry, the

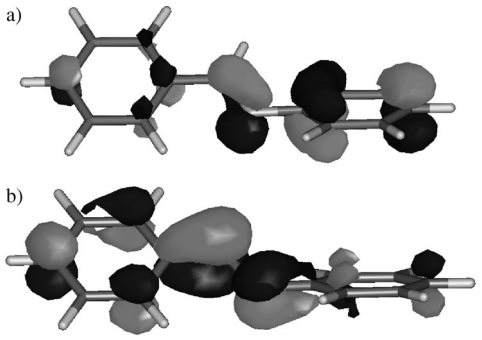

Figure 6. a) HOMO and b) LUMO Kohn–Sham orbitals of NBA (gas phase).

HOMO is also asymmetric and oriented towards the aniline ring. The LUMO has the largest coefficients at the imine bridge and at the benzylidene ring. As a consequence, a partial charge transfer from the N (right) to the C side (left) of NBA is expected upon photo-excitation. The second lowest-energy absorption signal in Figure 5 is caused by at least three transitions, most of them populating the π^* (LUMO) orbital from lower-lying occupied orbitals.

The position and oscillator strength of the lowest-lying absorption of the *trans* isomer depends on the solvent and more so on substituents. This is demonstrated by the results given in Table 8. In most cases the lowest-energy transition also has the largest oscillator strength, with the exceptions of NBA and TMNBA (Table 8).

From analysing the results given in Table 8, we note the following observations: Substituents shift the lowest-energy signal, almost always to the red. The shift is up to 58 nm, for **3** (4-OMe-4′-CN). The "partner species" **4** (4-CN-4′-OMe) shows only a small redshift of the HOMO→LUMO transition relative to NBA. All substituents lead to an increase in the oscillator strength. An exceptional case is **7** (TMNBA), which shows, due to steric effects, a distorted *trans* structure. As a consequence, the π system is not delocalised over two rings, causing a $\pi \rightarrow \pi^*$ transition that is strongly blueshifted.

Regarding solvent effects, we see that for NBA and alkyl-substituted species (**1**, **7**, and **8**), the effects are small. For all NBAs that are substituted with π donors and/or π acceptors, the effects of a solvent are more pronounced. Usually, the solvent causes a redshift. The largest shift occurs if a methoxy group is in the 4-position. For 4-OMe-4′-CN, for example, the solvent-induced redshift is 13 nm. A bigger effect of the solvent is found for oscillator strengths, which in almost all cases increase. Note that the differences between the three solvents (THF, acetone and methanol) are minor.

Table 8. Lowest-energy transitions of (substituted) *trans*-NBA molecules in different solvents: wavelengths (in nm) and oscillator strengths (in brackets).

		Gas	THF	Acetone	Methanol
1	4-Me-4′-Me	337 (0.42)	339 (0.60)	338 (0.60)	337 (0.59)
2	4-CN-4′-CN	358 (0.47)	360 (0.60)	359 (0.60)	359 (0.60)
3	4-OMe-4′-CN	389 (0.55)	402 (0.68)	401 (0.67)	400 (0.67)
4	4-CN-4′-OMe	335 (0.80)	343 (1.11)	343 (1.11)	342 (1.10)
5	4-Me-4′-CN	370 (0.44)	378 (0.58)	377 (0.57)	376 (0.57)
6	4-CN-4′-Me	332 (0.56)	335 (0.85)	334 (0.85)	333 (0.85)
7	TMNBA[a]	259 (0.52)	261 (0.72)	260 (0.71)	260 (0.70)
8	TBI	333 (0.38)	333 (0.51)	333 (0.50)	332 (0.50)
9	4-Me-4′-OMe	335 (0.53)	339 (0.76)	338 (0.76)	337 (0.75)
10	4-OMe-4′-OMe	347 (0.59)	353 (0.78)	353 (0.78)	352 (0.77)
11	4-OMe-4′-Me	349 (0.55)	354 (0.72)	353 (0.71)	353 (0.71)
12	NBA	331 (0.29)	331 (0.42)	330 (0.41)	330 (0.41)

[a] In the case of TMNBA, there is also a lower-energy absorption at around 370 nm, with a very small oscillator strength of 0.01–0.03 depending on the environment.

The absorption spectrum of the *cis* isomer of NBA is shown in Figure 5b. Apart from an emerging, very weak, low-energy feature at around 27 000 cm^{-1}, the most intense low-energy signal that dominates the spectrum shifts to the blue; to about 40 200 cm^{-1} (249 nm, 5.0 eV) in the gas phase. The corresponding transition is a complicated mixture of $n \rightarrow \pi^*$ and $\pi \rightarrow \pi^*$ excitations, involving several orbitals and partial charge transfer. The decrease of the features at around 30 000 cm^{-1} and increasing intensity at around 40 000 cm^{-1}, that is, the overall blueshift, is also in agreement with earlier experiments.[17,21]

An optimal optical switch should have distinct absorption energies for *cis* and *trans* forms and at the same time be thermally as stable as possible. For the imines studied herein, thermal stability can only be expected at sufficiently low temperatures. Figure 7 shows a plot of the energy difference $\Delta E = h\nu_c - h\nu_t$ (in which ν_c and ν_t are the frequencies of most intense low-energy transitions for *cis* and *trans*) versus the computed thermal *cis*→*trans* isomerisation rate (gas phase) at 213 K. It is recognised that the "optimal switches" with large ΔE values and small rates, are of the type 4-OMe-4′-X, namely, molecules with electron donors in the 4-position. The 4-OMe-4′-X compounds not only have the largest isomerisation barriers in the ground state, they are also those with the best photochromic behaviour. This finding may have implications for the design of optimal, imine-based molecular switches.

3. Summary and Conclusions

In this work a set of (substituted) NBAs in different solvents has been studied with respect to their switching ability. Most of the results are based on quantum chemistry, but a comparison with low-temperature NMR spectroscopy experiments was also given for the reaction rates. The most important results are summarized as follows:

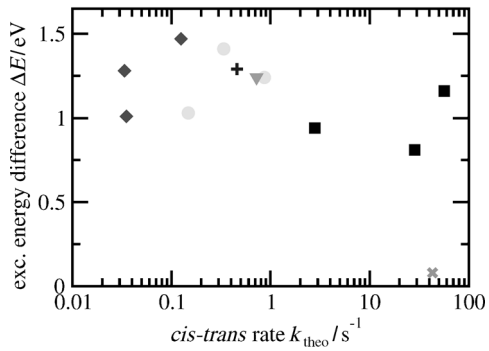

Figure 7. Electronic excitation energy differences, $\Delta E = h\nu_c - h\nu_t$, versus *cis*→*trans* thermal rate constants at 213 K. 4-CN-4′-X: ■, 4-Me-4′-X: ●, 4-OMe-4′-X: ◆, TMNBA: ×, TBI: +, and NBA: ▼.

1) NBA molecules are characterised by relatively low activation energies for the thermal *cis*→*trans* (back) reaction, resulting in thermally unstable compounds at room temperature. To arrive at thermally more stable *cis* isomers, one has to go to low temperatures (≈200 K) and/or attach π donors at electronically active positions of the aniline ring. Electronically active positions are *para* (4 and 4′) or *ortho* (2 and 2′), whereas *meta* positions are inactive due to small or zero coefficients in the frontier orbitals. Solvent effects were found to be comparatively small, in particular when compared with the effect of substituents.
2) The agreement between B3LYP/6-31G* theory and experiment is good as far as (*trans*-) geometries and/or UV/Vis spectra are concerned. For thermal isomerisation rates in solvents, the absolute theoretical values differ quite substantially from the experimental ones, with the former being several orders of magnitude larger than the latter. We attribute this deviation to a simplified treatment of the solvent, which can have an influence on Arrhenius prefactors and activation energies. Future theoretical work should try to improve on the solvent model.

The lower activation energy barrier of the thermal (back) *cis–trans* isomerisation of the imines shifts their applicability range to lower temperatures than those of azobenzenes. On the other hand, the low barrier may also be advantageous because it allows for rapid, reversible geometrical changes in light-driven molecular devices.[9,39] Furthermore, the imine group offers a broader variability in chemical and physical properties and its combination with azo units offers perspectives for new functionalities. It is therefore most worthwhile to consider aromatic imines as alternatives to azobenzene switches.

Acknowledgement

We acknowledge support by the Deutsche Forschungsgemeinschaft through SFB 658 on Elementary Processes in Molecular Switches at Surfaces, projects C2 and B7.

Keywords: density functional calculations · imines · isomerization · photochemistry · thermochemistry

[1] *CRC Handbook of Organic Photochemistry and Photobiology* (Eds.: F. Lenci, W. Horspool), CRC, Boca Raton, **2000**.
[2] S. D. Evans, S. R. Johnson, H. Ringsdorf, L. M. Williams, H. Wolf, *Langmuir* **1998**, *14*, 6436.
[3] D. Yang, M. Piech, N. S. Bell, D. Gust, S. Vail, A. A. Garcia, J. Schneider, C.-D. Park, M. A. Hayes, S. T. Picraux, *Langmuir* **2007**, *23*, 10864.
[4] F. L. Callari, S. Petralia, S. Conoci, S. Sortino, *New J. Chem.* **2008**, *32*, 1899.
[5] D. Liu, Y. Xie, H. Shao, X. Jiang, *Angew. Chem.* **2009**, *121*, 4470; *Angew. Chem. Int. Ed.* **2009**, *48*, 4406.
[6] M. Alemani, M. V. Peters, S. Hecht, K.-H. Rieder, F. Moresco, L. Grill, *J. Am. Chem. Soc.* **2006**, *128*, 14446.
[7] J. Henzl, M. Mehlhorn, K. Morgenstern, *Nanotechnology* **2007**, *18*, 495502.
[8] S. Hagen, F. Leyssner, D. Nandi, M. Wolf, P. Tegeder, *Chem. Phys. Lett.* **2007**, *444*, 85.
[9] J. M. Lehn, *Chem. Eur. J.* **2006**, *12*, 5910.
[10] a) H. B. Bürgi, J. D. Dunitz, *Helv. Chim. Acta* **1970**, *53*, 1747; b) K. Ezumi, H. Nakai, S. Sakata, K. Nishikida, M. Shiro, T. Kubota, *Chem. Lett.* **1974**, 1393.
[11] J. Bernstein, I. Izak, *J. Chem. Soc. Perkin Trans. 2* **1976**, 429.
[12] P. Skrabal, J. Steiger, H. Zollinger, *Helv. Chim. Acta* **1975**, *58*, 800.
[13] R. Akaba, K. Tokumaru, T. Kobayashi, *Bull. Chem. Soc. Jpn.* **1980**, *53*, 1993.
[14] M. Traetteberg, I. Hilmo, *J. Mol. Struct.* **1978**, *48*, 395.
[15] a) H. B. Bürgi, J. D. Dunitz, *J. Chem. Soc. D* **1969**, 472; b) K. Weiss, C. H. Warren, G. Wettermark, *J. Am. Chem. Soc.* **1971**, *93*, 4658; c) L. N. Patnaik, S. Das, *Int. J. Quantum Chem.* **1985**, *27*, 135.
[16] R. Kuhn, H. M. Weitz, *Chem. Ber.* **1953**, *86*, 1199.
[17] E. Fischer, Y. Frei, *J. Chem. Phys.* **1957**, *27*, 808.
[18] G. Wettermark, J. Weinstein, J. Sousa, L. Dogolioti, *J. Phys. Chem.* **1965**, *69*, 1584.
[19] U. Berns, G. Heinrich, H. Güsten, *Z. Naturforsch. B* **1976**, *31*, 9539.
[20] T. Asano, H. Furuta, H.-J. Hofmann, R. Cimiraglia, Y. Tsuno, M. Fujio, *J. Org. Chem.* **1993**, *58*, 4418.
[21] K. Maeda, K. A. Muszkat, S. Sharafi-Ozeri, *J. Chem. Soc. Perkin Trans. 2* **1980**, 1282.
[22] T. W. Swaddle, H. Doine, S. D. Kinrade, A. Sera, T. Asano, T. Okada, *J. Am. Chem. Soc.* **1990**, *112*, 2378.
[23] N. R. King, E. A. Whale, F. J. Davis, A. Gillbert, G. R. Mitchell, *J. Mater. Chem.* **1997**, *7*, 625.
[24] J. W. Lewis, C. Sandorfy, *Can. J. Chem.* **1982**, *60*, 1720.
[25] a) H. Kessler, *Angew. Chem.* **1970**, *82*, 237; *Angew. Chem. Int. Ed. Engl.* **1970**, *9*, 219; b) H. Kessler, *Tetrahedron* **1974**, *30*, 1861; c) H. Yamataka, S. C. Ammal, T. Asano, Y. Ohga, *Bull. Chem. Soc. Jpn.* **2005**, *78*, 1851.
[26] K. M. Tait, J. A. Parkinson, D. I. Gibson, P. R. Richardson, W. J. Ebenezer, M. G. Hutchings, A. C. Jones, *Photochem. Photobiol. Sci.* **2007**, *6*, 1010.
[27] *Gaussian 09* (*Revision A.02*), M. J. Frisch, G. W. Trucks, H. B. Schlegel, G. E. Scuseria, M. A. Robb, J. R. Cheeseman, G. Scalmani, V. Barone, B. Mennucci, G. A. Petersson, H. Nakatsuji, M. Caricato, X. Li, H. P. Hratchian, A. F. Izmaylov, J. Bloino, G. Zheng, J. L. Sonnenberg, M. Hada, M. Ehara, K. Toyota, R. Fukuda, J. Hasegawa, M. Ishida, T. Nakajima, Y. Honda, O. Kitao, H. Nakai, T. Vreven, J. A. Montgomery, Jr., J. E. Peralta, F. Ogliaro, M. Bearpark, J. J. Heyd, E. Brothers, K. N. Kudin, V. N. Staroverov, R. Kobayashi, J. Normand, K. Raghavachari, A. Rendell, J. C. Burant, S. S. Iyengar, J. Tomasi, M. Cossi, N. Rega, N. J. Millam, M. Klene, J. E. Knox, J. B. Cross, V. Bakken, C. Adamo, J. Jaramillo, R. Gomperts, R. E. Stratmann, O. Yazyev, A. J. Austin, R. Cammi, C. Pomelli, J. W. Ochterski, R. L. Martin, K. Morokuma, V. G. Zakrzewski, G. A. Voth, P. Salvador, J. J. Dannenberg, S. Dapprich, A. D. Daniels, O. Farkas, J. B. Foresman, J. V. Ortiz, J. Cioslowski, D. J. Fox, Gaussian, Inc., Wallingford, CT, **2009**.
[28] A. Becke, *J. Chem. Phys.* **1993**, *98*, 5648.
[29] R. Ditchfield, W. Hehre, J. Pople, *J. Chem. Phys.* **1971**, *54*, 724.
[30] H. Eyring, *Chem. Rev.* **1935**, *17*, 65.
[31] J. Dokić, M. Gothe, J. Wirth, M. Peters, J. Schwarz, S. Hecht, P. Saalfrank, *J. Phys. Chem. A* **2009**, *113*, 6763.

[32] C. Peng, H. Schlegel, *Isr. J. Chem.* **1993**, *33*, 449.
[33] C. Peng, P. Ayala, H. Schlegel, M. Frisch, *J. Comput. Chem.* **1996**, *17*, 49.
[34] N. Tanaka, Y. Xiao, A. C. Lasaga, *J. Atmos. Chem.* **1996**, *23*, 37.
[35] S. Miertuš, E. Scrocco, J. Tomasi, *Chem. Phys.* **1981**, *55*, 117.
[36] M. Casida, C. Jamorski, K. Casida, D. Salahub, *J. Chem. Phys.* **1998**, *108*, 4439.
[37] H. Kramers, *Physica* **1940**, *7*, 284.
[38] P. Hänggi, P. Talkner, M. Borkovec, *Rev. Mod. Phys.* **1990**, *62*, 251.
[39] E. R. Kay, D. A. Leigh, F. Zerbetto, *Angew. Chem.* **2007**, *119*, 72; *Angew. Chem. Int. Ed.* **2007**, *46*, 72.

Received: March 7, 2011
Published online on July 5, 2011

